

# BLIND ESTIMATION OF MIXED NOISE PARAMETERS IN IMAGES USING ROBUST REGRESSION CURVE FITTING

Victoria Zabrodina <sup>a</sup>, Sergey Abramov <sup>a</sup>, Vladimir Lukin <sup>a</sup>, Jaakko Astola <sup>b</sup>,

Benoit Vozel <sup>c</sup>, Kacem Chehdi <sup>c</sup>

<sup>a</sup> Department of Transmitters, Receivers and Signal Processing, National Aerospace University  
17 Chkalova st., 61070, Kharkov, Ukraine  
email: victoriya\_zabr@mail.ru, ask379@mail.ru, lukin@ai.kharkov.com  
web: k504.xai.edu.ua

<sup>b</sup> Institute for Signal Processing, Tampere University of Technology  
P.O. Box-553, FIN-33101, Tampere, Finland  
email: jta@cs.tut.fi  
web: ticsp.cs.tut.fi

<sup>c</sup> University of Rennes I  
Lannion cedex, BP 80518, France  
email: benoit.vozel@univ-rennes1.fr, kacem.chehdi@univ-rennes1.fr  
web: www.univ-rennes1.fr

## ABSTRACT

*Methods for blind estimation of signal dependent noise parameters from scatter-plots by polynomial regression are considered. Some new modifications as well as known ones are discussed and their performance is compared for test images with simulated signal dependent noise. Recommendations on method application and parameter setting are given.*

## 1. INTRODUCTION

Noise is one of the main factors degrading image quality in various applications [1, 2]. Because of this, noise presence should be taken into account for most image processing stages as filtering, edge detection, reconstruction, compression [3-5], etc. However, noise statistics is not always known in advance and it is desirable to estimate it from an image at hand [6, 7].

Although pure additive and pure multiplicative models of noise are still popular and are valid for some applications as SAR imaging [1, 4, 7], there is a current tendency to use more complex and adequate models of, in general, signal dependent (mixed) noise [6, 8, 9]. Such noise can be a mixture of additive and signal dependent (e.g., Poisson) components or additive and multiplicative. It might have even more specific behavior with maximal intensity for local means in the middle of dynamic range of image representation [9]. Then a task of blind estimation of noise statistics becomes complicated and leads to necessity of fitting regression curves into scatter-plots of local estimates of noise variance vs. local mean.

There are numerous methods of regression curves fitting into scatter-plots but in blind estimation of mixed noise statistics this fitting should be robust [6, 7, 9-11]. This deals

with the fact that scatter-plots of local estimates of noise variance in small sized blocks (scanning windows) usually contain outliers obtained in heterogeneous image blocks that belong to edges, fine details and texture. Note that local estimates can be obtained in both spectral and spatial domains. The spectral domain techniques perform better for highly textural images but they produce biased estimation for spatially correlated noise. In turn, for spatial domain estimates, there can be more outliers for highly textural images but normal estimates (obtained in homogeneous image regions) are less sensitive to (unknown) spatial correlation of noise [3]. Thus, since spatial domain methods can be considered more universal, we will focus on analyzing them below.

Within the general approach to solving the considered task of mixed noise parameter estimation from scatter-plots, there are quite many variants. For example, a scatter-plot can be obtained either for all positions of blocks or only for those ones somehow recognized as homogeneous. Then, a polynomial of the corresponding (model-based) order is fitted into scatter-plot and the polynomial parameters are accepted as estimates of statistical parameters of mixed noise. In the simplest case of mixed additive and multiplicative noise, one needs to fit polynomial  $Y = a + bX$  where  $Y = \hat{\sigma}_{loc}^2$ ,  $X = \hat{\bar{I}}_{loc}^2$  where  $\hat{\sigma}_{loc}^2$  and  $\hat{\bar{I}}_{loc}$  are local variance and local mean estimates in a block. This model of mixed noise relates to, e.g., radar images [12]. Another example is the model  $Y = a + bX$  where  $X = \hat{\bar{I}}_{loc}$ . It is commonly accepted for noise in component images formed by hyperspectral sensors [8, 13]. Then  $\mathbf{a}$  and  $\mathbf{b}$  are accepted as estimates of the signal-independent (additive) noise variance and the parameter characterizing signal dependent noise component, respectively.

To improve accuracy of estimation, detection of homogeneous blocks can be carried out at preliminary stage of scatter-plot forming. This can be done in different ways, for example, by preliminary rejection of outliers [13] or by pre-segmentation based method [14]. However, in any case, these methods are unable to remove all heterogeneous blocks and a scatter-plot contains abnormal local estimates. Even if a scatter-plot is formed with such pre-processing, regression polynomial fitting should be carried out using robust methods.

Robustness at this stage can be provided in the following manner: 1) robust fitting using all points of a scatter-plot; 2) robust or non-robust fitting using some reference points that correspond to scatter-plot cluster centers determined in robust manner. This paper deals with comparison analysis for several modified and known fitting methods from the viewpoint of resulting accuracy of the blind estimation of mixed noise parameters. The study is carried out for mixed additive and multiplicative noise although the results are important for other types of signal-dependent noise.

## 2. DESCRIPTION OF THE BASIC TECHNIQUE

The basic stages of the methods considered below are the following: 1) image pre-segmentation based on the method [15] able to perform in condition of unknown noise type and characteristics; 2) detection of homogeneous fragments and blocks by post-processing the obtained segmented image [14]; 3) calculation of local variance estimates and squared local mean estimates in blocks of size 7x7 as recommended in [14]; 4) scatter-plot forming; 5) regression line fitting.

The initially considered methods of regression line fitting are the following: 1) robust determination of cluster centers and LMS fitting where a) LMS fitting can be used and b) weighted LMS (WLMS) can be applied [11]; 2) robust fitting (RLMS) using all points of a scatter-plot (function RobustFit in MathLab [10]) without any pre-processing.

## 3. INITIAL STATISTICAL EXPERIMENT DESCRIPTION

Simulations for some artificial (RSA) and other test images (Barbara, Baboon) have been carried out first. Without losing generality, the model for mixed additive and multiplicative noise  $I_{ij} = I_{ij}^{\text{tr}} \cdot \mu_{ij} + n_{ij}$  was used. Here  $I_{ij}^{\text{tr}}$  denotes

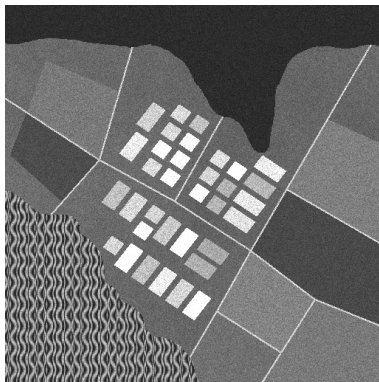


Figure 1 - Noisy test image RSA

noise-free image,  $\mu_{ij}$  defines multiplicative noise component obeying Gaussian distribution with unity mean and relative variance  $\sigma_{\mu}^2$ , and  $n_{ij}$  describes additive noise component with zero mean Gaussian distribution with variance  $\sigma_a^2$ . For the model given in Introduction,  $\sigma_{\mu}^2$  corresponds to parameter b and  $\sigma_a^2$  to parameter a, respectively.

As a quantitative criteria, the estimation bias  $\Delta_x = \left| \langle \hat{\sigma}_x^2 \rangle - \sigma_x^2 \right|$ , variance  $\theta_x^2 = \left\langle \left( \hat{\sigma}_x^2 - \langle \hat{\sigma}_x^2 \rangle \right)^2 \right\rangle$

and aggregate error  $\varepsilon_x = \Delta_x^2 + \theta_x^2$  have been used. Sub-index x denotes belonging of the corresponding parameter for additive (a) or multiplicative ( $\mu$ ) noise. Notation  $\langle \bullet \rangle$  means averaging by realizations. To provide statistically stable results the number of realizations was 100.

The simulated values are  $\sigma_a^2 = 10$ ,  $\sigma_{\mu}^2 = 0.01$ . They have been chosen from the earlier experience for side-look aperture radar images [12] and the estimates of parameters a and b for sub-band images of AVIRIS data [16].

### 3.1 Analysis of preliminary results

For artificial test image RSA (that contains quite many large area homogeneous regions, see its noisy version with aforementioned variances in Fig. 1), all considered methods perform rather well with providing small bias and variance for both estimated parameters. The best results are provided by LMS method, especially for multiplicative component. The results for RMLS fitting are worse and for the WLMS methods the results are the worst (although the accuracy for all three methods is appropriate).

For middle-texture test image (Barbara), all methods produce approximately the same bias for additive component, the minimal estimation variance is provided by the RLMS method. For multiplicative component, the best results are produced by the WLMS method.

For highly texture image (Baboon), all methods exhibit poorer accuracy for both components. The best characteris-

Table 1 – Simulated results for initially considered robust fitting methods

Noise parameters: $\sigma_a^2 = 10$ , $\sigma_{\mu}^2 = 0.01$							
Image	Method	$\Delta_a$	$\theta_a^2$	$\varepsilon_a$	$\Delta_{\mu}$	$\theta_{\mu}^2$	$\varepsilon_{\mu}$
RSA	LMS	0.091	0.027	0.03	-3.2e-05	1.9e-08	2.0e-08
	RLMS	0.098	0.01	0.02	-2.8e-04	1.0e-08	8.8e-08
	WLMS	0.23	0.12	0.16	-3.6e-04	5.0e-08	1.7e-07
Barbara	LMS	10.3	9.1	114.3	7.8e-05	7.3e-08	7.9e-08
	RMLS	9.8	2.6	98.2	-2.1e-04	3.3e-08	7.9e-08
	WLMS	7.37	9.7	64.0	-2.7e-06	4.0e-08	4.0e-08
Baboon	LMS	68.4	81.2	4761	1.0e-03	2.3e-07	1.3e-06
	RLMS	36.4	76.9	1400	-1.3e-04	2.3e-07	2.4e-07
	WLMS	56.5	35.6	3223	-6.4e-04	9.0e-08	5.0e-07

tics are, in general, provided by RLMS; however, WMLS produces smaller variances of estimation. The worst accuracy is produced by LMS. It is worth noting that providing high accuracy for textural images is the most crucial task.

Thus, the LMS method performs well enough for quite simple test images but fails for highly textural ones. Therefore, in the remainder part let us consider two other, robust fitting, techniques to analyze are they able to provide better accuracy of estimation for mixed noise parameters.

### 3.2 Analysis of reasons of estimation bias for the method WLMS

The scatter-plot analysis (see Fig. 2) shows that some reference points (cluster centers shown by red squares) are considerably biased with respect to the corresponding true positions (the true dependence is shown by black). The sizes of these clusters can be rather large. Thus, the assigned weights in WLMS fitting are large too [11]. This leads to biased estimation of mixed noise parameters. Therefore, more robust regression techniques are to be used. Within the considered approach to estimation of mixed noise parameters, the final accuracy depends both on accuracy of initial local estimates and correctness of regression curve fitting. In this paper, we focus on accuracy analysis of the latter stage.

## 4. PROPOSED SOLUTIONS AND THEIR PERFORMANCE ANALYSIS

### 4.1 Considered and proposed methods

There exists a robust fitting method Ransac (RSC) [17]. Its basic idea is to fit regression lines using two randomly used reference points, to calculate the number of reference points that are in consensus (that belong to confidence interval) for each formed regression line, selection of the maximal subset of reference points that are in consensus, obtaining regression for this subset by LMS method.

Let us give some details of the confidence interval determination in our case. Initially the confidence interval is determined for one reference point for which the distance to regression line corresponds to median distance for all reference points. The confidence interval is calculated inversely

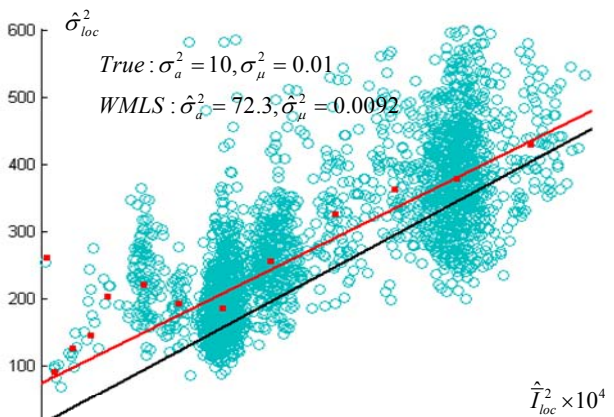


Figure 2 – Scatter-plot for the test image Baboon and approximation lines: true one (black) and automatically obtained one (red)

proportionally to the number of points in the corresponding scatter-plot cluster (the cluster sizes are known after pre-segmentation). Based on the estimated confidence interval for starting point, prediction for other reference points under assumption of multiplicative noise and pre-estimated line slope is done (see limits of the obtained confidence intervals indicated by two black dashed lines in Fig. 3). Due to presence of multiplicative component in mixed noise, confidence intervals become larger for larger arguments of cluster points. The use of such censoring allows rejecting “outlying” reference points and improving fitting accuracy.

The RSC method has certain drawbacks. First, it has one tuned parameter to be set for determining the confidence interval for the starting point. Depending upon mixed noise characteristics, optimal value of this parameter  $k_{RSC}$  (that provides minimal aggregate errors) varies from 7 to 9 (optimal values of  $k_{RSC}$  are presented in Table 2 after slash). One more drawback of the RSC method is that quite many cluster centers can be removed (see Fig. 3 where 7 cluster centers are outside the confidence interval).

To partly alleviate this shortcoming, we have proposed a modified method called AntiRansac (ARSC). Its basic idea is to perform initial regression using WLMS method [11] with further rejection of points outside the confidence interval and carrying out further, final, regression for the obtained trimmed set of reference points, also using WLMS. The confidence interval is determined as for the RSC method using the pre-estimated slope (Fig. 4). In contrast to the RSC, the confidence interval determination is carried out only one time. This accelerates processing. For the example in Fig. 4, three outlying reference points have been rejected.

We have also designed a regression method called double weighting (DWLMS). The basic idea is to fit regression line by the WLMS method [11], then to correct weights by setting them inversely proportional to distances of cluster centers to the fitted line, then to fit the line finally using the WMLS with the corrected weights (Fig. 5).

### 4.2 Analysis of the obtained results

The obtained simulation results are collected in Table 2 for

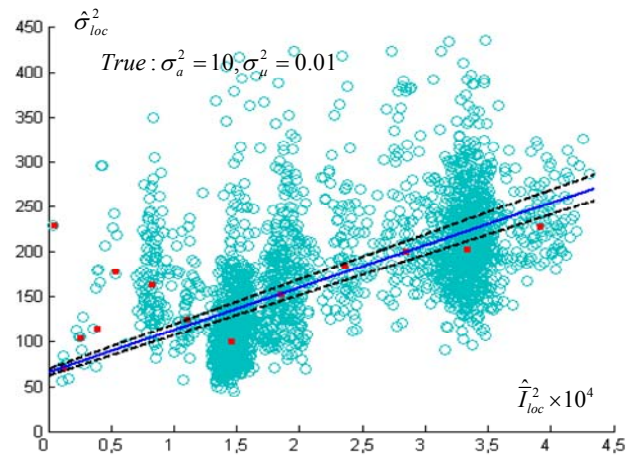


Figure 3 – Scatter-plot for the test image Baboon and the curve fitted for two reference points (blue) and confidence interval limits (black dashed)

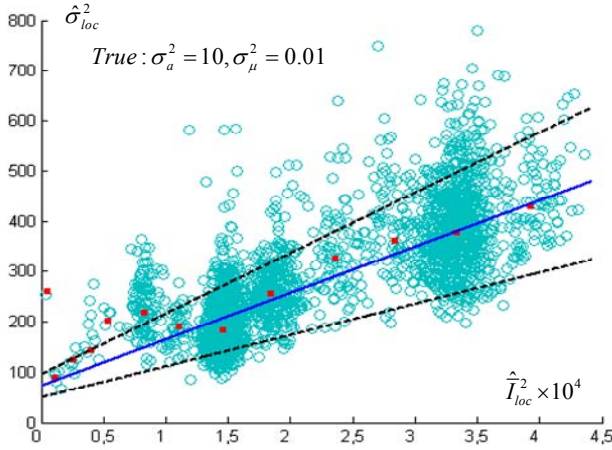


Figure 4 – Scatter-plot for the test image Baboon and the curve fitted for all reference points (blue) and confidence interval limits (black dashed)

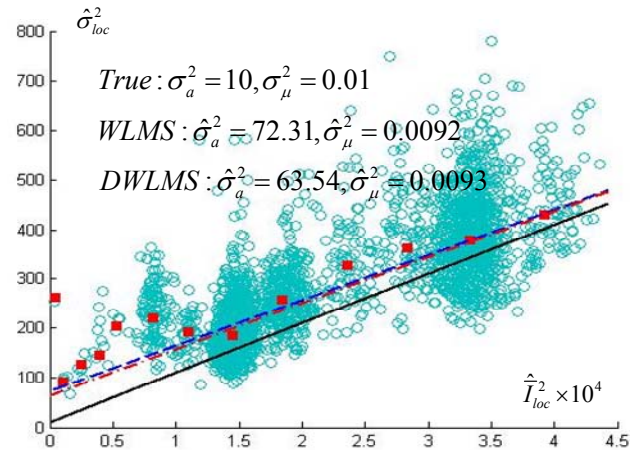


Figure 5 – Scatter-plot for the test image Baboon and curves: true (black solid), fitted by WLMS (blue dashed) and fitted by DWLMS (red dot-dashed)

three considered test images and two combinations of mixed noise parameters. It is seen that for the RSA artificial test image the best results are provided by the RLMS and DWLMS methods in the sense of the smallest  $\varepsilon_a$  and  $\varepsilon_\mu$ .

For additive component, the RLMS accuracy is slightly better but it is slightly worse for multiplicative component. The method WLMS produces larger variance of estimation compared to the DWLMS and RLMS. The method ARSC pro-

duces good accuracy as well, but slightly worse than the method DWLMS. Bias for both components is almost negligible for all methods and both combinations of mixed noise parameters. Variance and aggregate error are also acceptable for practical application (it is desirable to have relative errors  $\varepsilon_x^{\text{rel}} = \sqrt{\varepsilon_x} / \sigma_x^2$  about few percent [3]).

For the test image Barbara, the best results are provided by the proposed method DWLMS, it is better than RLMS in

Table 2 – Simulated results for all considered robust fitting methods

Image	Parameters	Method	$\Delta_a$	$\theta_a^2$	$\varepsilon_a$	$\Delta_\mu$	$\theta_\mu^2$	$\varepsilon_\mu$
RSA	$\sigma_a^2 = 10$ $\sigma_\mu^2 = 0.005$	RLMS	0.0181	0.0080	0.0083	-1.1e-04	4.8e-09	1.7e-08
		WLMS	0.094	0.0312	0.040	-1.8e-04	1.0e-08	5.0e-08
		RSC / 7	0.0199	0.031	0.0315	-1.4e-04	1.0e-08	3.0e-08
		ARSC	0.038	0.027	0.028	-1.5e-04	1.0e-08	3.0e-08
		DWLMS	-0.086	0.0069	0.014	-9.3e-05	1.0e-09	1.0e-08
	$\sigma_a^2 = 100$ $\sigma_\mu^2 = 0.05$	RLMS	1.02	0.84	1.89	-2.3e-03	5.9e-07	5.9e-06
		WLMS	-0.93	3.64	4.50	-1.6e-03	1.4e-06	3.9e-06
		RSC / 9	-1.27	3.84	5.45	-1.4e-03	1.5e-06	3.3e-06
		ARSC	-1.28	2.48	4.12	-1.4e-03	9.6e-07	2.8e-06
		DWLMS	-1.63	0.71	3.35	-1.3e-03	3.8e-07	2.0e-07
Barbara	$\sigma_a^2 = 10$ $\sigma_\mu^2 = 0.005$	RLMS	6.15	1.01	38.84	4.3e-05	1.3e-08	1.5e-08
		WLMS	5.85	3.75	37.93	1.4e-04	1.0e-08	3.0e-08
		RSC / 7	6.34	7.94	48.09	8.0e-05	4.0e-08	4.0e-08
		ARSC	6.25	4.93	44.03	8.3e-05	2.0e-08	3.0e-08
		DWLMS	4.77	0.17	22.92	2.0e-04	1.0e-09	4.0e-08
	$\sigma_a^2 = 100$ $\sigma_\mu^2 = 0.05$	RLMS	23.27	78.6	619.87	-1.9e-03	1.0e-06	4.6e-06
		WLMS	10.82	76.37	193.41	-1.0e-03	6.0e-07	1.6e-06
		RSC / 8	6.47	170.64	212.50	-8.6e-04	1.0e-06	1.8e-06
		ARSC	7.13	337.06	387.96	-8.1e-04	1.3e-06	2.0e-06
		DWLMS	6.22	9.38	48.05	-7.6e-04	2.5e-07	8.3e-07
Baboon	$\sigma_a^2 = 10$ $\sigma_\mu^2 = 0.005$	RLMS	31.35	30.26	1012.9	8.0e-05	8.1e-08	8.7e-08
		WLMS	53.56	15.04	2883.25	-5.6e-04	3.0e-08	3.4e-07
		RSC / 9	63.47	450.35	4478	-8.6e-04	4.8e-07	1.2e-06
		ARSC	34.08	38.77	1200.1	1.2e-04	7.0e-08	8.0e-08
		DWLMS	36.84	20.56	1377.53	-1.5e-04	5.0e-08	7.0e-08
	$\sigma_a^2 = 100$ $\sigma_\mu^2 = 0.05$	RLMS	80.05	1248.6	7656.2	-2.6e-03	3.5e-06	1.0e-05
		WLMS	62.83	625.26	4573.1	-1.5e-03	1.8e-06	4.1e-06
		RSC / 7	62.52	654.21	4563	-1.4e-03	1.8e-06	3.9e-06
		ARSC	49.85	974.19	3459.70	-1.1e-03	2.3e-06	3.6e-06
		DWLMS	62.67	346.78	4274.71	-1.6e-03	1.1e-06	3.8e-06



the sense of all or almost all analyzed quantitative criteria. The accuracy of the WLMS method is also good enough. The methods RSC and ARSC are characterized by performance comparable to the WLMS.

The estimates of additive noise component variance are considerably biased. To our opinion, the main reason for this is self-noise of this test image. Similar effects have been recently reported for the test image Lena [18]. Because of this, requirement to estimation accuracy is not satisfied for additive component. However, for multiplicative component the relative errors are of the order few percent.

For the test image Baboon (see Table 2), the best results in terms of aggregate errors are, in general, provided by the proposed methods ARSC and DWLMS. Considerable bias of additive noise variance estimation is observed for all methods. To our opinion, this happens due to highly textural character of this test image that leads to positive bias of original local estimates of noise variance. The multiplicative noise variance is estimated with high enough accuracy (slightly worse than for the test image Barbara). The worst estimation accuracy is observed for the method RSC (for less intensive noise) and the method RLMS (for more intensive noise).

Summarizing analysis for three test images, it is possible to state that for simple structure images (RSA) all considered methods perform well enough. For images with more complex structure, especially highly textural ones, the benefits of the proposed methods ARSC and DWLMS clearly appear themselves in less biased estimation. Since we do not know in advance how complex is an analyzed image, it is worth using more universal methods, e.g., DWLMS. In practice, it might be reasonable to apply restrictions imposed on estimates of mixed noise parameters as, e.g., non-negativity of both estimates.

## 5. GENERAL CONCLUSIONS

It is demonstrated that accuracy of blind estimation of mixed noise parameters can be sufficiently improved by more advanced methods of robust curve fitting into scatter-plot. The proposed DWLMS method, in general, possesses quite good accuracy. In some cases, especially for textural images, considerable bias of additive noise variance estimates is observed. One of the main reasons is the influence of local image content on original local estimates of noise variance in blocks. It seems problematic to eliminate this drawback by only modifying the fitting procedure. To our opinion, it is worth trying to analyze or to design methods for decreasing bias of original local estimates. This can be one possible direction of our future studies.

## REFERENCES

- [1] W.K. Pratt, *Digital Image Processing*, 4-th Edition, NY, USA, Wiley-Interscience, 2007.
- [2] C. Oliver, S. Quegan, *Understanding Synthetic Aperture Radar Images*, SciTech Publishing, 2004.
- [3] B. Vozel, S. Abramov, K. Chehdi, V. Lukin, N. Ponomarenko, M. Uss, J. Astola, *Blind methods for noise evaluation in multi-component images*, Book chapter in *Multivariate Image Processing*, France, 2009.
- [4] L. Sendur, I.W. Selesnick, "Bivariate shrinkage with local variance estimation," *IEEE Signal Processing Letters*, Vol. 9, No 12, pp. 438-441, 2002.
- [5] M.C. Motwani, M.C. Gadiya, R.C. Motwani, F.C. Harris, "Survey of Image Denoising Techniques," *Proc. of GSP 2004*, Santa Clara, CA, Sept 27-30, 2004.
- [6] A. Foi, M. Trimeche, V. Katkovnik, K. Egiazarian, "Practical Poissonian-Gaussian Noise Modeling and Fitting for Single Image Raw Data," *IEEE Transactions on Image Processing*, vol. 17, No 10, pp. 1737-1754, 2007.
- [7] B. Aiazzi, L. Alparone, S. Baronti, Reliably "Estimating the Speckle Noise from SAR Data," *Proceedings of IGARSS*, 1999, pp. 1546-1548.
- [8] J.P. Kerekes, J.E. Baum, "Hyperspectral Imaging System Modeling," *Lincoln Laboratory Journal*, Vol. 14, No 1, pp. 117-130, 2003.
- [9] C. Liu, R. Szeliski, S.B. Kang, C.L. Zitnick, W. T. Freeman, "Automatic estimation and removal of noise from a single image," *IEEE Transactions on Pattern Analysis and Machine Intelligence*, Vol. 30, No 2, pp. 299-314, 2008.
- [10] DuMouchel, W. and F. O'Brien, "Integrating a Robust Option into a Multiple Regression Computing Environment," in *Computing Science and Statistics: Proceedings of the 21st Symposium on the Interface*, (K. Berk and L. Malone, eds.), American Statistical Association, Alexandria, VA, pp. 297-301, 1989.
- [11] S.K. Abramov, V.V. Zabrodina, V.V. Lukin, B. Vozel, K. Chehdi, J. Astola, "Improved method for blind estimation of the variance of mixed noise using weighted LMS line fitting algorithm," *Proceedings of ISCAS*, Paris, France, June 2010, pp. 2642-2645.
- [12] V. Lukin, N. Ponomarenko, S. Abramov, B. Vozel, K. Chehdi, "Improved noise parameter estimation and filtering of MM-band SLAR images," *Proc. of MSMW 2007*, Kharkov, Ukraine, 2007, Vol. 1, pp. 439-441.
- [13] B. Aiazzi, L. Alparone, A. Barducci, S. Baronti, P. Marcoinni, I. Pippi, and M. Selva, "Noise modelling and estimation of hyperspectral data from airborne imaging spectrometers," *Annals of Geophysics*, Vol. 49, No. 1, Feb 2006.
- [14] V. Lukin, S. Abramov, B. Vozel, K. Chehdi, J. Astola, "Segmentation-based method for blind evaluation of noise variance in images," *SPIE Journal on Applied Remote Sensing*, Vol. 2, 15 p., Aug. 2008, open access paper.
- [15] Klaine L., Vozel B., Chehdi K., "Unsupervised Variational Classification Through Image Multi-Thresholding", *Proceedings of the 13th EUSIPCO Conference*, 2005, 4 p., Antalya, Turkey.
- [16] V. Lukin, S. Abramov, N. Ponomarenko, M. Uss, M. Zriakhov, B. Vozel, K. Chehdi, J. Astola, "Methods and automatic procedures for processing images based on blind evaluation of noise type and characteristics," *Journal of Applied Remote Sensing*, Vol. 5, 26 p., 2011.
- [17] Fischler, M.A. and R.C. Rolles, "Random Sample Consensus: A Paradigm for Model Fitting with Applications to Image Analysis and Automated Cartography". *Commun. ACM*. Vol. 24, No.6, pages 381-395, 1981.
- [18] D. Zoran, Y. Weiss, "Scale invariance and noise in natural images," *Proceedings of IEEE 12th International Conference on Computer Vision*, 2009, pp. 2209-2216.